Medicine®

Activin B signaling may promote the conversion of normal fibroblasts to scar fibroblasts

Shi-Kang Deng, MD[a], Jian-Zhong Tang, MM[a], Yan Jin, MB[a], Ping-Hai Hu, MD[a], Jun-Feng Wang, MB[a], Xiao-Wen Zhang, MD[b],*

Abstract

This study is to explore the molecular mechanism of benign bile duct hypertrophic scar formation.

Differential proteins between the normal fibroblast (NFB) and scar fibroblast (SCFB) were screened by protein chip assay, and analyzed by pathway-enrichment analysis and function-enrichment analysis. The differential proteins were further tested by ELISA. SiRNA-Act B was transfected to SCFB to down-regulate the expression of Act B. NFB was incubated with rh-Act B. The cell apoptosis and cell cycle were determined by flow cytometry. The expression of Act B, Smad2/3, transforming growth factor-β1 (TGF-β1), endothelin-1 (ET-1), thrombospondin-1 (Tsp-1), and Oncostatin M (OSM) were detected by Western blot.

A total of 37 differential proteins were identified in SCFBs by microarray ($P < .05$), including 27 up-regulated proteins and 10 down-regulated proteins ($P < .05$). Their function were associated with Activin signaling, synthesis and degradation of extracellular matrix, formation and activation of cytokine, inflammatory reaction, immunoreaction, tissue damage reaction, cell cycle, migration, apoptosis, and secretion, etc. ELISA results showed that the expression of Act B, TGF-β1, ET-1 were higher in SCFBs, while the expression of Tsp-1 and OSM were lower in SCFBs ($P < .05$). After interfered by siRNA-Act B, the expression of Act B mRNA decreased ($P < .05$). The percentage of early apoptosis increased ($P < .05$). The expression of Act B, Smad2/3, TGF-β1 were decreased and Tsp-1, OSM were increased ($P < .05$). After treatment with rh-Act B, the percentage of G0/G1 phase of NFBs was decreased and that of S phase was increased without significance ($P > .05$). The expression of Act B, Smad2/3, TGF-β1 were increased ($P < .05$) and Tsp-1, OSM were decreased ($P < .01$).

There are differentially expressed proteins between SCFBs and NFBs. Activin B signal plays an important role in the process of NFB transforming to SCFB, and TGF-β1, Smad2/3, Tsp-1, and OSM are important participants.

Abbreviations: BBS = Benign bile duct scar, MAPKs = serine/threonine protein kinase, MFB = myofibroblast ofibroblast, NFB = normal fibroblast, SCFB = scar fibroblast, TGF-β1 = transforming growth factor-β1.

Keywords: activin, benign bile duct scar, fibroblast, transforming growth factor-β1

1. Introduction

Benign bile duct scar (BBS) is very common in biliary surgery. Due to the deep location of the bile duct, BBS is very difficult to be treated with either topical drug administration or surgery.[1] Although in some patients, obstruction caused by BBS can be remove by surgery, there is still scar recurrence after surgery in some patients, not only causing pain to patients, but also great challenges to the biliary surgeons.[2] Therefore, BBSs have attracted increasing attention by biliary surgeons.

The main pathological changes of BBSs are bile duct scar contracture and scar stenosis. Bile duct healing is accompanied by inflammation and macrophage accumulation, which continuously synthesize and secrete transforming growth factor-β1 (TGF-β1).[3] TGF-β1 is a potent mitogen and scarring factor. It can stimulate fibroblasts to proliferate and to express α-actin (α-SMA),[4] thus transforming into myofibroblast (MFB),[4] which can secrete extensive extracellular matrix such as collagen, fibronectin, and proteoglycans.[5] Inhibition of stromal collagen degradation and deposition of collagen will result in bile duct scar formation and contracture.[6] Hyperplasia of scar tissue may cause the bile duct stenosis, unsmooth bile drainage, and cholestasis in liver.[7] And, the toxic bile acids may damage liver cells, causing liver atrophy and hyperplasia, followed by cholestatic cirrhosis, portal hypertension, liver failure, and other severe pathological changes.[8,9]

Activin (Act) is a glycoprotein hormone firstly isolated from ovary, and belongs to the TGF-β superfamily.[10] Act has three

molecular subtypes of Act A, Act B, and Act AB, and their receptors are ActRIA, ActRIB, ActRII A, and ActRIIB.[11] Acts exert their biological functions through the serine/threonine protein kinase (MAPKs) signaling pathways.[12,13] Studies have found that the Act expression levels are abnormally elevated in mouse skin lesions, especially during granulation tissue formation and in hyperproliferative tissues. The transient over-expression of Act may play a positive role in the healing process of tissue and organ wounds.[14–16] However, if the expression of Act is consistently high, it will lead to the occurrence of fibrosis of tissues and organs.[17] Some research-ers[18,19] have found that overexpression of Act in the transgenic mice could promote skin damage repair, but the scar tissues were quickly developed at the lesions, forming skin scars.

Herein, we screened the differential proteins between the normal tissue-derived and scar tissue-derived fibroblasts by protein chip assay. The effects of Act B on the other differential proteins in fibroblasts were also investigated. The study will provide experimental evidence for the clinical research and treatment of bile duct hypertrophic scars.

2. Materials and methods

2.1. Sample collection

The bile duct scar tissues and the surrounding normal bile duct tissues were from 22 patients with intrahepatic bile duct stones (8 men and 14 women; age 28–45 years old). Informed consent was obtained and the study was approved by the ethics review board of Kunming Medical University.

2.2. Isolation and culture of primary fibroblasts

The tissues were placed in a petri dish, rinsed 3 times with PBS to remove the blood, bile, and stones, and soaked in the medium containing penicillin and streptomycin for 30 minutes. The tissues were cut into pieces of about 1 mm × 1 mm in size. Then the tissue pieces were attached to a culture flask. The moisture on the tissues was dried to make the tissue pieces better adhere to the tissue flask. When the water on the tissue pieces was dried, complete medium was carefully added to just overwhelm the tissue pieces. The culture flask was placed in an atmosphere containing 5% CO_2 at 37°C, and the medium was changed every 3 days. The isolated primary normal fibroblast (NFB) and scar fibroblast (SCFB) were cultured in complete medium at 37 and 5% CO_2.

2.3. Protein chip assay

The NFB and SCFB cells were collected when the confluency was >80% and lysed in a lysing buffer containing protease inhibitors on ice for 30 minutes. The cell lysates were centrifuged at 14,000 rpm for 15 minutes at 4°C. The supernatants were dialyzed to PBS (pH = 8.0) at 4°C. The dialysis buffer was changed every 3 hours for three times. The protein concentration was deter-mined by a bicinchoninic acid (BCA) method, and then the proteins were labeled with biotin.

RayBio AAH-BLG-1 Kit (RayBiotech, Norcross, GA) was used. Briefly, glass chips were equilibrated for 20 to 30 minutes and dried for 1 to 2 hours at room temperature. To each well of the chip, 400 μL blocking solution was added and incubated for 30 minutes. After removing the blocking solution, 400 μL sample solution was added into each well and incubated overnight at 4°C. After that, the sample solution was discarded and washed

with washing solution I (RayBiotech, Norcross, GA) 4 times (5 minutes each time) and washing solution II (RayBiotech, Norcross, GA) 3 times (5 minutes each time). The samples were stained with Cy3 (RayBiotech, Norcross, GA) and incubated for 2 hours at room temperature in the dark, and then washed again. The fluorescence of samples was detected by an Axon GenePix laser scanner system (RayBiotech, Norcross, GA). The images were quantitatively analyzed by the AAH-BLG-1 data analysis software (RayBiotech, Norcross, GA). The differentially expressed proteins were screened based on signal values more than 100 and Fold change more than 1.5 or less than 0.66, after removing the background by selecting Normalization 2.

2.4. Differential protein analysis

The GO annotations of the differential proteins were performed using online tool (http://www.geneontology.org). Using the DAVID Bioinformatics Resources (National Institutes of Health, MD, USA), the GO functional annotations and biological pathway analysis of the differential proteins were carried out, and the enrichment classes of the related functions of the differential proteins were obtained.

2.5. ELISA

The bile duct scar tissues and normal bile duct tissues were lysed with RIPA (containing protease inhibitors) on ice bath for 30 minutes, and then centrifuged at 14,000 rpm for 15 minutes at 4°C. The supernatant was collected. The samples were added to a 96-well plate and incubated for 2.5 hours at room temperature. After that, biotin-labeled antibodies were added and incubated for 1 hour. Then, streptavidin was added and incubated for 45 minutes. Color development was conducted with tetramethyl-benzidine (TMB). The absorbance at 450 nm was measured with a plate reader (Bio-Rad Laboratories Inc., Hercules, CA).

2.6. SiRNA transfection

SNFB cells were seeded into a 24-well plate at a concentration of 1×10^5/well, and incubated for 24 hours. Then, 1.25 μL of the siRNA of Act B (20 μM) (siRNA-Activin B kit, Guangzhou RiboBio Co., Ltd., Guangzhou, China) was diluted with 50 μL 1× riboFECT^TM CP buffer (riboFECTTMCP transfection re-agent, Guangzhou RiboBio Co., Ltd., Guangzhou, China) and incubated at room temperature for 5 minutes. Then, 5 μL riboFECT^TM CP reagent (riboFECTTMCP transfection reagent, Guangzhou RiboBio Co., Ltd., Guangzhou, China) was added and mixed. The mixture was mixed with 443.75 μL cell culture media, added to the cells and incubated for 48 hours. The transfection efficiency was observed under an inverted fluores-cence microscope (Olympus Co., Tokyo, Japan).

2.7. Reverse transcription PCR

The total RNA of cells was extracted with Trizol, and the concentration was determined by absorbance at 260 nm. The RNA was reverse transcribed into cDNA, and the target genes were amplified with a reverse transcription Polymerase Chain Reaction (RT-PCR) Reverse Transcription Kit (Thermo Fisher Scientific Inc., Waltham, MA) using the following condition: pre-denaturation at 94°C for 5 minutes, followed by 35 cycles of denaturation at 94°C for 1 minute, annealing at 53°C for

1 minute and extension at 72 °C for 1 minute, and final extension at 72 °C for 10 minutes. The Polymerase Chain Reaction (PCR) product was then detected by agarose gel electrophoresis and visualized by a Gel Imaging System (Bio-Rad Laboratories, CA). The optical density of each band was measured by Image J software (National Institutes of Health, MD, USA).

2.8. Recombinant human Act B (rh-ActB) protein incubation with the normal fibroblasts

The NFB were seeded into a 6-well plate at 1×10^5 cells/well. After cell adhesion overnight, the medium was changed with fresh medium containing 10 ng/mL rh-Act B (PeproTech, Inc., Rocky Hill, NJ), and cultured for another 48 hours. The cells were collected for the detection of cell cycle and expression of differentially expressed proteins.

2.9. Flow cytometry

After 72 hours of siRNA Act B transfection, the cells were collected, re-suspended with pre-cooled PBS and fixed with pre-cooled 70% ethanol at 4 °C. After 24 hours, the cells were centrifuged at 1000 rpm for 5 minutes, and then re-suspended with pre-cooled PBS. The cells were stained with popidium iodide (PI) for 30 minutes at 37 °C in the dark. Flow cytometry was used to detect the cell cycle. The results were analyzed by ModFit software (Verity Software House, ME, USA) (Version 3.1).

For the detection of cell apoptosis, the cells were collected as described above and stained with Annexin V-FITC and PI before flow cytometry analysis.

2.10. Western blot

After 48 hours of transfection/overexpression, cells were collected and lysed with cell lysing buffer containing protease inhibitors on ice. The lysate was centrifuged at 14,000 rpm for 15 minutes at 4 °C, and the supernatant was collected. After determining the protein concentration, the sample was subjected to polyacrylamide gel electrophoresis (SDS-PAGE) and transferred to a Poly vinylidene fluoride (PVDF) membrane. The membrane blocked with 5% skimmed milk for 1 hour. Then, the membrane was incubated with primary antibodies (mouse anti-human) of Act B, endothelin-1 (ET-1), thrombospondin-1 (Tsp-1), TGF-β1, Oncostatin M (OSM), and Smad2/3 (Santa Cruz, CA) overnight at 4 °C. After washing, the membrane was incubated with the secondary antibody at room temperature for 1 hour. The membrane was finally colored with chemiluminescence reagent. The protein bands were visualized in a gel imager (Bio-Rad Laboratories Inc., Hercules, CA).

2.11. Statistical analysis

The statistical analysis was performed with the statistical software SPSS 17.0 (SPSS Inc., Chicago, IL). Measurement data are expressed as mean ± standard deviation (SD). For normally distributed data, t test was used for the comparison between 2 independent samples, and one-way analysis of variance (ANOVA) was used for multi-sample comparisons. For the non-normally distributed data, Wilcoxon rank sum test was used for the comparison of 2 samples, while Kruskal-Wallis rank sum test was used for the comparison of multiple samples. A P value <.05 was considered as statistically significant.

Table 1

Representative differential proteins by protein chip analysis.

Protein name	NFB	SCFB	Fold change
Activin B	167	256	1.536
Activin RII A/B	109	169	1.554
Angiopoietin-like 2	268	508	1.898
BTC	158	269	1.701
CD30/TNFRSF8	885	454	0.513
CD40/TNFRSF5	108	212	1.965
D6	137	222	1.620
Endostatin	115	180	1.569
Endothelin	301	1,300	4.321
FGF-7/KGF	138	215	1.561
FGF-18	266	445	1.677
FLRG	118	179	1.517
GDF9	1942	2,967	1.528
GFR alpha-4	789	1,364	1.729
Growth Hormone (GH)	1739	558	0.321
IGFBP-rp1/IGFBP-7	972	426	0.439
IL-1 F9/IL-1 H1	1225	628	0.513
IL-1 R4/ST2	114	186	1.627
IL-1 R9	522	291	0.557
IL-6	1011	1539	1.523
IL-6 R	145	221	1.532
IL-17B	154	301	1.963
IL-18 R alpha/IL-1 R5	283	155	0.548
IL-19	9046	5911	0.653
IL-24	119	184	1.548
Insulin R	1439	2451	1.703
I-TAC/CXCL11	223	355	1.594
MCP-1	1065	1829	1.718
MCP-3	143	235	1.649
M-CSF	244	119	0.489
MMP-15	124	204	1.650
MMP-20	322	869	2.703
OSM	1317	840	0.638
OX40 Ligand/TNFSF4	638	1,103	1.728
TGF-beta 1	706	1,149	1.628
Thrombospondin-1	1180	253	0.214
TNF-beta	928	1474	1.589

Note: Fold change = SCFB signal/NFB signal. NFB = normal fibroblast, SCFB = scar fibroblast.

3. Results

3.1. Identification and analysis of differential proteins

Protein chip analysis of 507 proteins in NFB and SCFB, was performed. According to the criteria of signal value >100, fold change >1.5 or <.66, a total of 37 differential proteins were identified. Compared with NFBs, there were 27 up-regulated proteins and 10 down-regulated proteins in SCFBs. Among them, levels of TGF-β1 and endothelin were increased in SCFB cells (Table 1), compared with NFB cells.

In order to demonstrate the pathways and functions of the differential proteins, DAVID software was used to analyze these proteins. A total of 18 pathway enrichment (corrected P-value <.05) (Table 2) and 195 functional enrichment (correlated P-value <.05) (Table 3) were found.

Pathway enrichment analysis (Table 2) revealed that the differentially expressed proteins were mainly involved in cytokine–cytokine receptor binding, JAK-STAT signaling pathway, chemokine and chemokine receptor binding, activin signaling pathway, collagen degradation signaling pathway, PI3K-Akt signaling pathway, TNF signaling pathways, TGF-β

Table 2

Enrichment analysis of different protein pathways.

Pathway-enrichment	Corrected P-value	$-\log10^{(\text{Corrected } P\text{-value})}$
Cytokine-cytokine receptor interaction	2.67E–16	15.573783
Jak-STAT signaling pathway	0.000206	3.685568
Chemokine receptors bind chemokines	0.000704	3.152338
Signaling by Activin	0.003216	2.492632
Rheumatoid arthritis	0.004725	2.325553
IL23-mediated signaling events	0.008775	2.056772
Malaria	0.008991	2.046173
Platelet degranulation	0.013890	1.857307
Extracellular matrix organization	0.014714	1.832283
Response to elevated platelet cytosolic Ca^{2+}	0.015366	1.813431
Collagen degradation	0.018201	1.739911
PI3K-Akt signaling pathway	0.019373	1.712810
TNF signaling pathway	0.022407	1.649617
Peptide ligand-binding receptors	0.025901	1.586680
TGF-beta signaling pathway	0.026877	1.570619
TGF-beta signaling pathway	0.045121	1.345620
Insulin/IGF pathway-mitogen activated protein kinase kinase/MAP kinase cascade	0.046525	1.332318
Degradation of the extracellular matrix	0.047238	1.325707

Corrected P-value < .05, the higher of $-\log10^{(\text{Corrected } P\text{-value})}$ value, the more relevant.

signaling pathways, insulin/insulin-like growth factor signaling pathways, and extracellular matrix degradation signaling pathway.

Functional enrichment analysis (Table 3) revealed that differential proteins were mainly involved in the synthesis and degradation of extracellular matrix, cytokine production and activation, inflammatory immune responses, tissue injury responses, cell cycle, cell proliferation, cell migration, cell viability, apoptosis, cell secretion, activin binding, and collagen synthesis and degradation.

The above results suggest that the differential-proteins-involved biological processes and molecular functions may be closely related to the occurrence and development of scars. In both the pathway enrichment and functional enrichment analysis, activin was involved.

3.2. Verification of the proteins related to the scar formation

To verify the identified proteins related to the scar formation, ELISA was performed. In general, the expressions of Act B, TGF-β1, ET-1, Tsp-1, and OSM were in consistent with the protein chip analysis. The levels of Act B (130.80±58.46 pg/mL vs 88.83±51.01 pg/mL) (Fig. 1A), TGF-β1 (10.31±4.45 ng/mL vs 5.18±2.68 ng/mL) (Fig. 1B) and ET-1 (107.63±18.04 pg/mL vs 59.75±12.49 pg/mL) (Fig. 1C) in the scar tissues were significantly higher than those of the normal tissues ($P < .05$). However, compared with normal tissues, the levels of Tsp-1 (672.42±193.56 ng/mL vs 1311.47±278.05 ng/mL) (Fig. 1D) and OSM (296.49±72.28 pg/mL vs 485.52±78.91 pg/mL) (Fig. 1E) in the scar tissues were significantly lower ($P < .05$). These results indicate that the changing trends of the identified proteins are consistent with the results of protein chip assay.

3.3. The effect of downregulation of Act B on the cell apoptosis

To detect whether the transfection of siRNA-Act B was successful, cell fluorescence was observed. After the siRNA-Act

B was transfected into SCFB, the transfected cells showed red fluorescence under a fluorescence microscope (Fig. 2A). Then, the mRNA level of Act B was determined by RT-PCR. As shown in Fig. 2B, Act B mRNA was significantly decreased in cells transfected with siRNA Act B than control ($P < .01$). This indicates that the siRNA-Act B was successfully transfected into the SCFBs.

Cell apoptosis of SCFB was detected after the transfection of siRNA-Act B. The percentage of early apoptosis in the siRNA-Act B group was 15.72±1.33%, which was significantly increased compared with that of the control group (0.32±0.02%) ($P < .01$) (Fig. 3). The percentage of late apoptosis in the siRNA-Act B group was 0.96±0.06%, which was also significantly higher than that of the control group (0.08±0.02%) ($P < .01$) (Fig. 3). This demonstrates that interference of the expression of Act B in SCFB increases the cell apoptosis.

3.4. The effect of downregulation of Act B on the expressions of related proteins of SCFB

After transfection of siRNA-Act B, the expressions of Smad2/3, TGF-β1, ET-1, Tsp-1, and OSM in SCFB were detected by Western blot. For the siRNA-Act B group, the expressions of Act B, Smad2/3, TGF-β1, and ET-1 decreased, among which the reduction of Act B, Smad2/3, and TGF-β1 was significant compared with the normal group ($P < .05$) (Fig. 4). In addition, the expressions of Tsp-1 and OSM in the siRNA-Act B group increased compared with the normal group ($P < .05$) (Fig. 4). These results indicate that the interference of the expression of Act B in the scar fibroblasts can reverse the expression of related proteins.

3.5. The effect of rh-Act B on the cell cycle of NFB

To determine the effect of Act B on cell cycle, flow cytometry was performed. After treatment with rh-Act B, the percentage of G0/G1 phase and G2/M phase of the NFBs decreased and the percentage in S phase increased in the ActB overexpression group, compared with control group, but the differences were not

Table 3

Enrichment analysis of different protein functions.

Function-enrichment	Corrected P-value	-log10(Corrected P-value)
Extracellular space	3.75E–09	8.425447
Cytokine activity	5.42E–09	8.265922
Extracellular region part	5.67E–07	6.246682
Inflammatory response	4.95E–05	4.305240
Cytokine receptor binding	4.95E–05	4.305240
Cytokine receptor activity	6.00E–05	4.221516
Positive regulation of response to external stimulus	0.000166	3.780124
Receptor binding	0.000206	3.685568
Growth factor activity	0.000206	3.685568
Cytokine production	0.000564	3.249072
Immune response	0.000704	3.152338
Extracellular region	0.000877	3.056825
Regulation of cytokine production	0.000950	3.023176
Chemokine activity	0.001363	2.865639
Positive regulation of cell proliferation	0.001363	2.865639
Response to wounding	0.001400	2.853806
Positive regulation of multicellular organismal process	0.001792	2.746689
Chemokine receptor binding	0.001859	2.730724
Interleukin-1 receptor activity	0.002281	2.641877
Positive regulation of chemotaxis	0.002821	2.549611
Positive regulation of cytokine production	0.002821	2.549611
Regulation of cell proliferation	0.003216	2.492632
Positive regulation of cell migration	0.004232	2.373412
Positive regulation of behavior	0.004232	2.373412
Positive regulation of cell motility	0.004408	2.355757
Positive regulation of cellular component movement	0.004686	2.329233
Positive regulation of locomotion	0.004986	2.302293
Regulation of cell migration	0.005269	2.278275
JAK-STAT cascade	0.005622	2.250145
Ossification	0.005622	2.250145
Tyrosine phosphorylation of STAT protein	0.006327	2.198821
Regulation of cell motility	0.007243	2.140073
Defense response	0.007437	2.128576
Regulation of chemotaxis	0.007437	2.128576
Positive regulation of leukocyte chemotaxis	0.007758	2.110270
Platelet alpha granule lumen	0.008293	2.081264
Protein kinase B signaling cascade	0.008293	2.081264
Regulation of response to external stimulus	0.008293	2.081264
Positive regulation of protein kinase B signaling cascade	0.008527	2.069184
Regulation of odontogenesis	0.008527	2.069184
Positive regulation of protein phosphorylation	0.008589	2.066066
Response to oxygen-containing compound	0.008754	2.057777
Regulation of locomotion	0.008991	2.046173
Positive regulation of phosphorylation	0.009042	2.043750
Transmembrane receptor protein serine/threonine kinase signaling pathway	0.009701	2.013194
Cytokine binding	0.009837	2.007150
Regulation of leukocyte chemotaxis	0.010498	1.978909
Leukocyte activation	0.010825	1.965588
Immune system process	0.010825	1.965588
Positive regulation of leukocyte migration	0.010825	1.965588
Platelet alpha granule	0.011399	1.943139
Regulation of cellular component movement	0.011399	1.943139
Response to external stimulus	0.011477	1.940165
Myeloid leukocyte activation	0.011615	1.934971
Peptidyl-tyrosine phosphorylation	0.011903	1.924348

(*continued*)

Table 3

(continued).

Function-enrichment	Corrected P-value	-log10(Corrected P-value)
Peptidyl-tyrosine modification	0.012072	1.918213
Positive regulation of cell division	0.012072	1.918213
Response to progesterone stimulus	0.012633	1.898489
Secretory granule lumen	0.012633	1.898489
Regulation of mononuclear cell proliferation	0.012791	1.893107
Positive regulation of leukocyte activation	0.013890	1.857307
Regulation of leukocyte proliferation	0.014714	1.832283
Positive regulation of protein kinase activity	0.014714	1.832283
Tyrosine phosphorylation of Stat3 protein	0.014746	1.831313
Regulation of behavior	0.014746	1.831313
Positive regulation of cell activation	0.015603	1.806780
Positive regulation of phosphate metabolic process	0.015603	1.806780
Positive regulation of phosphorus metabolic process	0.015603	1.806780
Regulation of polysaccharide biosynthetic process	0.015699	1.804125
Positive regulation of response to stimulus	0.015781	1.801869
Response to ketone	0.015781	1.801869
Response to hormone stimulus	0.015970	1.796686
Cellular response to oxygen-containing compound	0.016239	1.789437
activin receptor signaling pathway	0.016239	1.789437
Cellular response to endogenous stimulus	0.016239	1.789437
Intracellular protein kinase cascade	0.016239	1.789437
Vesicle lumen	0.016239	1.789437
Positive regulation of mononuclear cell proliferation	0.016239	1.789437
Cytoplasmic membrane-bounded vesicle lumen	0.016239	1.789437
Positive regulation of kinase activity	0.016250	1.789142
Regulation of peptidyl-tyrosine phosphorylation	0.017051	1.768255
Regulation of protein kinase B signaling cascade	0.017622	1.753947
Positive regulation of leukocyte proliferation	0.017622	1.753947
Regulation of polysaccharide metabolic process	0.018201	1.739911
T-helper 1 type immune response	0.018201	1.739911
Cell activation	0.018281	1.737994
Regulation of immune system process	0.018381	1.735636
Positive regulation of transferase activity	0.018445	1.734132
Platelet degranulation	0.019373	1.712810
Positive regulation of fibroblast migration	0.019373	1.712810
Positive regulation of odontogenesis	0.019373	1.712810
Regulation of mononuclear cell migration	0.019373	1.712810
Regulation of leukocyte activation	0.019373	1.712810
Cell proliferation	0.019432	1.711484
Regulation of leukocyte migration	0.019507	1.709814
Regulation of protein phosphorylation	0.022407	1.649617
Growth factor binding	0.022407	1.649617
Regulation of cell division	0.022804	1.641988
Cellular response to lipopolysaccharide	0.022804	1.641988
Response to endogenous stimulus	0.022804	1.641988
Positive regulation of isotype switching	0.022804	1.641988
Positive regulation of tumor necrosis factor Biosynthetic process	0.022804	1.641988
Regulation of macrophage chemotaxis	0.022804	1.641988
Regulatory T cell differentiation	0.022804	1.641988
Positive regulation of endothelial cell apoptotic process	0.022804	1.641988

(*continued*)

Table 3

(continued).

Function-enrichment	Corrected P-value	-log10(Corrected P-value)
Cellular response to organic substance	0.023055	1.637235
Regulation of tyrosine phosphorylation of STAT protein	0.024027	1.619306
Mononuclear cell proliferation	0.025012	1.601854
Cellular response to molecule of bacterial origin	0.025012	1.601854
Regulation of multicellular organismal process	0.025901	1.586680
Receptor complex	0.025901	1.586680
Regulation of cell activation	0.025901	1.586680
Regulation of intracellular protein kinase cascade	0.025901	1.586680
Regulation of interleukin-12 production	0.025901	1.586680
Mononuclear cell migration	0.025901	1.586680
Positive regulation of macrophage activation	0.025901	1.586680
Regulation of odontogenesis of dentin-containing tooth	0.025901	1.586680
Regulation of natural killer cell chemotaxis	0.025901	1.586680
Positive regulation of DNA recombination	0.025901	1.586680
Positive regulation of protein modification process	0.025901	1.586680
Cytokine biosynthetic process	0.026877	1.570619
Interleukin-12 production	0.026877	1.570619
Leukocyte proliferation	0.026877	1.570619
Adaptive immune response based on somatic recombination of immune receptors built from immunoglobulin superfamily domains	0.026877	1.570619
Odontogenesis	0.027598	1.559118
Cytokine metabolic process	0.027598	1.559118
Secretion by cell	0.028154	1.550456
Collagen metabolic process	0.028154	1.550456
Positive regulation of peptidyl-tyrosine Phosphorylation	0.028154	1.550456
Regulation of phosphorylation	0.028294	1.548300
Cellular response to biotic stimulus	0.028577	1.543979
Positive regulation of glycogen biosynthetic process	0.028577	1.543979
activin binding	0.028577	1.543979
Natural killer cell chemotaxis	0.028577	1.543979
Regulation of fibroblast migration	0.028577	1.543979
Negative regulation of immune system process	0.029934	1.523834
Multicellular organismal macromolecule metabolic process	0.030514	1.515504
Response to lipopolysaccharide	0.030514	1.515504
Heparin binding	0.031621	1.500026
Cellular response to chemical stimulus	0.032262	1.491307
Response to monosaccharide stimulus	0.032344	1.490206
Enzyme linked receptor protein signaling pathway	0.032344	1.490206
T-helper 1 cell differentiation	0.032344	1.490206
regulation of immunoglobulin secretion	0.032344	1.490206
Insulin-like growth factor receptor binding	0.032344	1.490206
CCR chemokine receptor binding	0.032344	1.490206
Regulation of localization	0.032376	1.489778
Positive regulation of protein metabolic process	0.032376	1.489778
Adaptive immune response	0.034154	1.466555
Bone development	0.034911	1.457035

(continued)

Table 3

(continued).

Function-enrichment	Corrected P-value	-log10(Corrected P-value)
Response to molecule of bacterial origin	0.035833	1.445720
Response to alcohol	0.036691	1.435437
positive regulation of glycogen metabolic process	0.036927	1.432659
Regulation of isotype switching	0.036927	1.432659
Positive regulation of MAPK cascade	0.037342	1.427799
Response to vitamin	0.038885	1.410213
G-protein coupled receptor binding	0.038885	1.410213
Regulation of protein secretion	0.038885	1.410213
Multicellular organismal metabolic process	0.038885	1.410213
Extracellular matrix organization	0.038885	1.410213
Positive regulation of protein serine/threonine kinase activity	0.039095	1.407884
Extracellular structure organization	0.039095	1.407884
Positive regulation of transmembrane receptor protein serine/threonine kinase signaling pathway	0.039095	1.407884
Positive regulation of inflammatory response	0.039095	1.407884
Negative regulation of cell migration	0.039095	1.407884
Regulation of lymphocyte proliferation	0.039095	1.407884
Positive regulation of activated T cell proliferation	0.039095	1.407884
Fibronectin binding	0.039095	1.407884
Regulation of tumor necrosis factor Biosynthetic process	0.039095	1.407884
Tumor necrosis factor biosynthetic process	0.039095	1.407884
Regulation of lymphocyte chemotaxis	0.039095	1.407884
Tyrosine phosphorylation of Stat1 protein	0.039095	1.407884
Behavioral response to pain	0.039095	1.407884
Platelet activation	0.039623	1.402054
leukocyte chemotaxis	0.040114	1.396708
Regulation of biomineral tissue development	0.041903	1.377756
Regulation of carbohydrate biosynthetic process	0.041903	1.377756
Negative regulation of cytokine production	0.042394	1.372694
Negative regulation of cell motility	0.042394	1.372694
Positive regulation of cellular protein metabolic process	0.042420	1.372430
Response to carbohydrate stimulus	0.043045	1.366079
Response to heat	0.043045	1.366079
Fibroblast migration	0.043045	1.366079
Response to mechanical stimulus	0.044319	1.353412
Response to organic substance	0.044525	1.351395
Negative regulation of cellular component movement	0.046525	1.332318
Response to steroid hormone stimulus	0.046525	1.332318
Regulation of production of molecular mediator of immune response	0.046525	1.332318
Granulocyte chemotaxis	0.046525	1.332318
Macrophage chemotaxis	0.047003	1.327878
Immunoglobulin secretion	0.047003	1.327878
Regulation of interleukin-17 production	0.047003	1.327878
Polysaccharide biosynthetic process	0.048104	1.317816
Secretion	0.048462	1.314600

Corrected P-value <.05, the higher of −log10(Corrected P-Value) value, the more relevant.
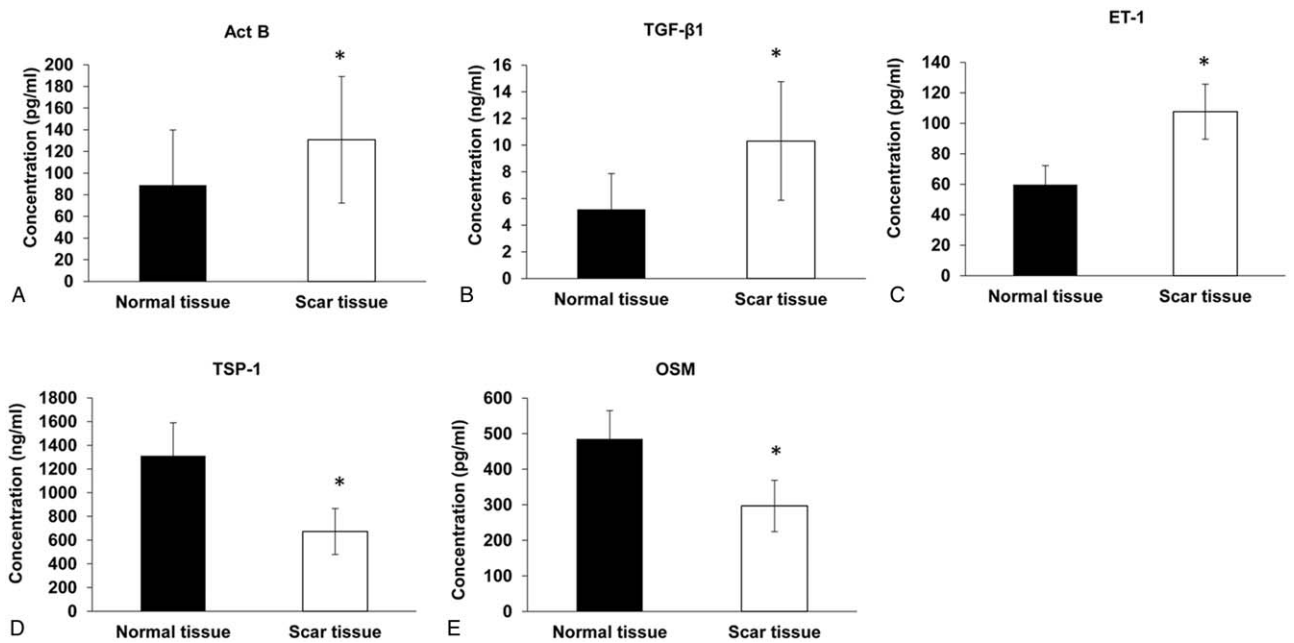
Figure 1. The expression of related proteins tested by ELISA. (A) Act B; (B) TGF-β1; (C) ET-1; (D) Tsp-1; (E) OSM. $^*P < .05$, compared with the NFBs. ET-1 = endothelin-1; NFB = normal fibroblast; OSM = Oncostatin M, TGF-β1 = transforming growth factor-β1; Tsp-1 = thrombospondin-1.
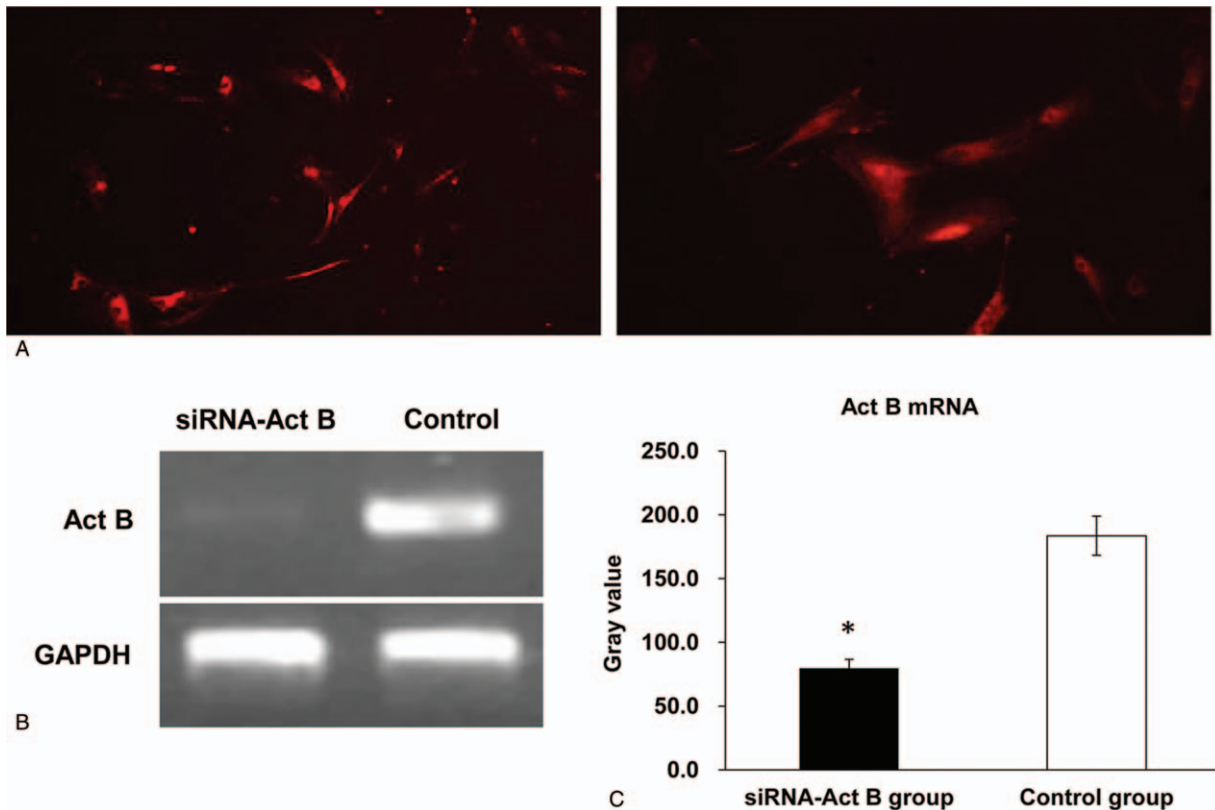

Figure 2. Knockdown of Act B by siRNA-Act B. The SCFBs were transfected with siRNA-Act B to down-regulate the expression of Act B. (A) The SCFBs observed under a fluorescence microscope after siRNA-Act B transfection. Magnification: 100×. (B) The expression of Act B mRNA after siRNA-Act B transfection detected by RT-PCR, and GAPDH was used as internal standard. (C) The relative value of Act B mRNA in the siRNA Act B group and the Control group. $^*P < .05$, compared with the Control group. GAPDH = glyceraldehyde-3-phosphate dehydrogenase, SCFB = scar fibroblast.
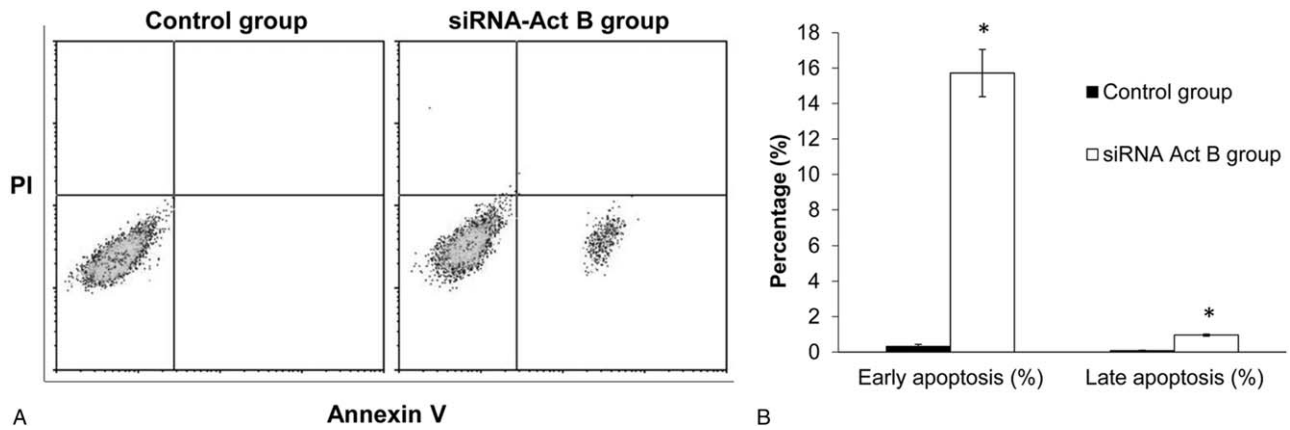
Figure 3. The effect of Act B interference on the apoptosis of SCFBs. (A) Cell apoptosis was detected by flow cytometry. (B) The percentage of cells at early and late apoptosis phases in the siRNA-Act B interfering group and the Control group. *$P < .05$, compared with the Control group. SCFB = scar fibroblast.

significant ($P > .05$) (Fig. 5). This indicates that overexpression of Act B in fibroblasts may not affect the proliferation.

3.6. The effect of rh-Act B on the related protein expressions of NFB

To determine the effect of rh-Act B expression on the protein levels of Act B, Smad2/3, TGF-β1, ET-1, Tsp-1, and OSM in NFB, Western blot was performed. After treated with rh-Act B, NFBs showed increased expressions of Act B, Smad2/3, TGF-β1, and ET-1 compared with the untreated NFBs, among which the

differences in Act B, Smad2/3, and TGF-β1 were significant ($P < .05$) (Fig. 6). In addition, the levels of Tsp-1 and OSM were significantly lower than those of the control group ($P < .01$) (Fig. 6). This suggests that rh-Act B treatment of the normal fibroblasts can reverse the expression of related proteins.

4. Discussion

Fibroblasts in normal skin and scar tissues had different sub-structures,[20,21] and they are very active in scar tissues.[22] Study[23] has shown that the fibroblasts of the normal dermis and
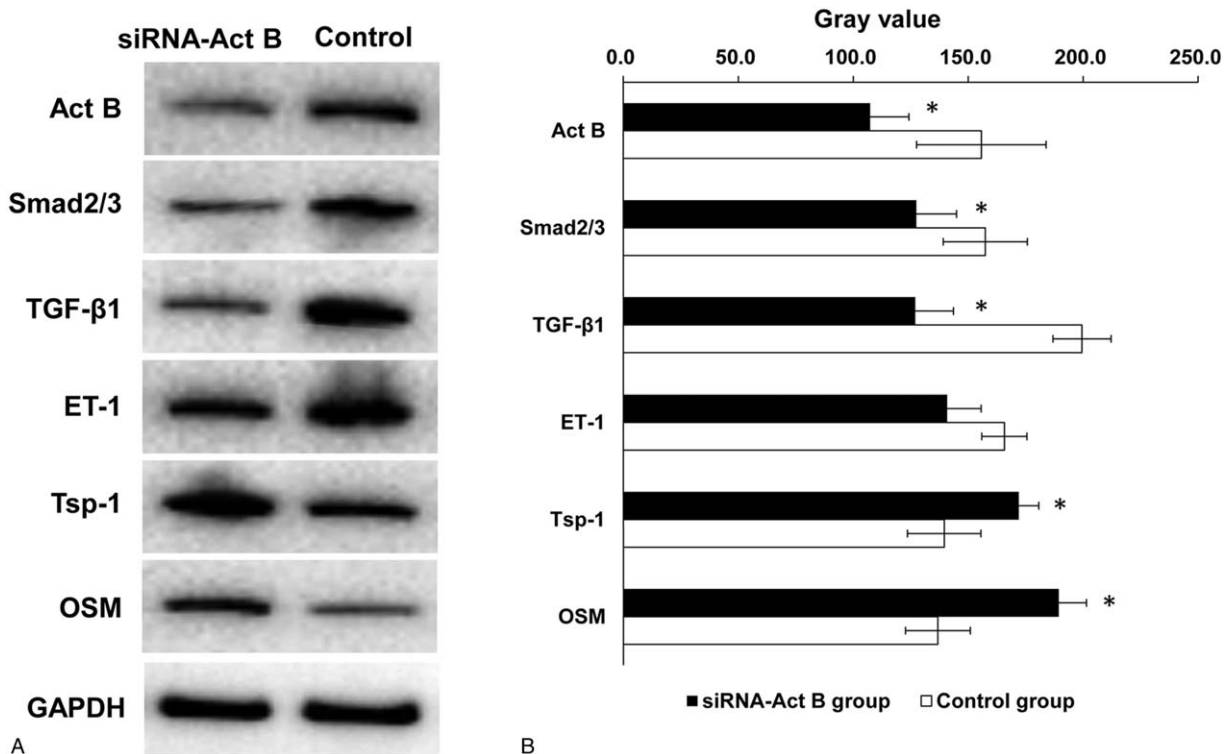

Figure 4. The effect of Act B interference on the protein expression. Western blot was used to detect protein expression. (A) Representative Western blot results. (B) The gray values of the protein bands. *$P < .05$, compared with control group.
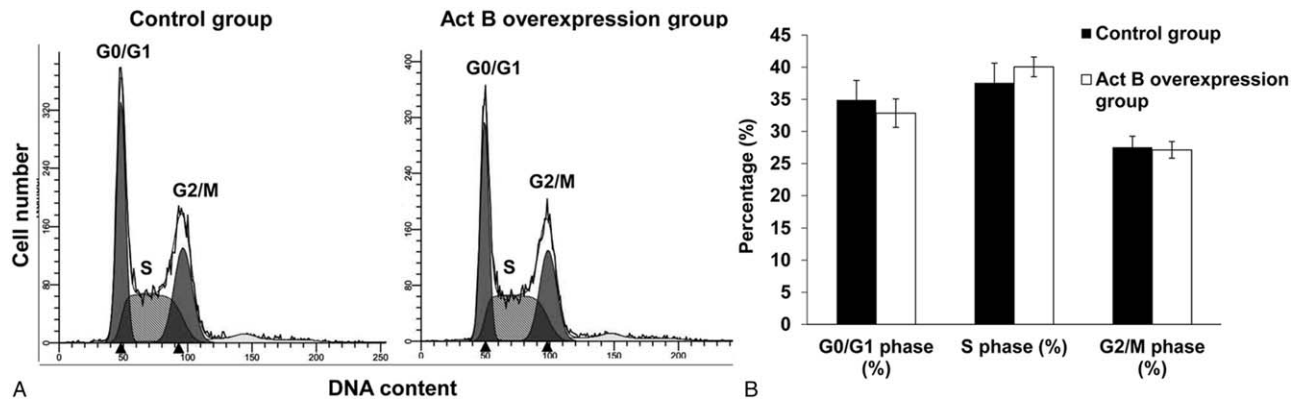
Figure 5. The effect of Act B overexpression on the cell cycle. (A) Representative flow cytometry results of the control group and the Act B overexpression group. (B) The percentage of cells at different phases in the Act B over-expression group and the Control group.

hypertrophic scars are heterogeneous, and these subpopulations are different in cell morphology, cell proliferation, collagen synthesis, growth factors, cytokine production, and involvement in inflammatory reactions. However, there are no specific protein markers for differentiating normal and scar fibroblasts, so they cannot be identified effectively.

Protein chip is a high-throughput rapid protein detection technology developed in recent years and has been used in basic research, clinical diagnosis, treatment, and prognosis of many diseases.[24] This study used this technology to screen the differential proteins between normal bile duct fibroblasts and

benign bile duct scar fibroblasts. Totally, 37 differential proteins were identified, including 27 up-regulated proteins and 10 down-regulated proteins. Their function were associated with signaling by Activin, synthesis and degradation of extracellular matrix, formation and activation of cytokine, inflammatory reaction, immunoreaction, tissue damage reaction, cell cycle, migration, apoptosis, and secretion, etc.

TGF-β1 is currently the most recognized and the most important scar factor.[25,26] It can increase vascularization, induce migration of fibroblasts, monocytes, and macrophages to the site of injury and promote fibrosis at the injury site.[6] It has
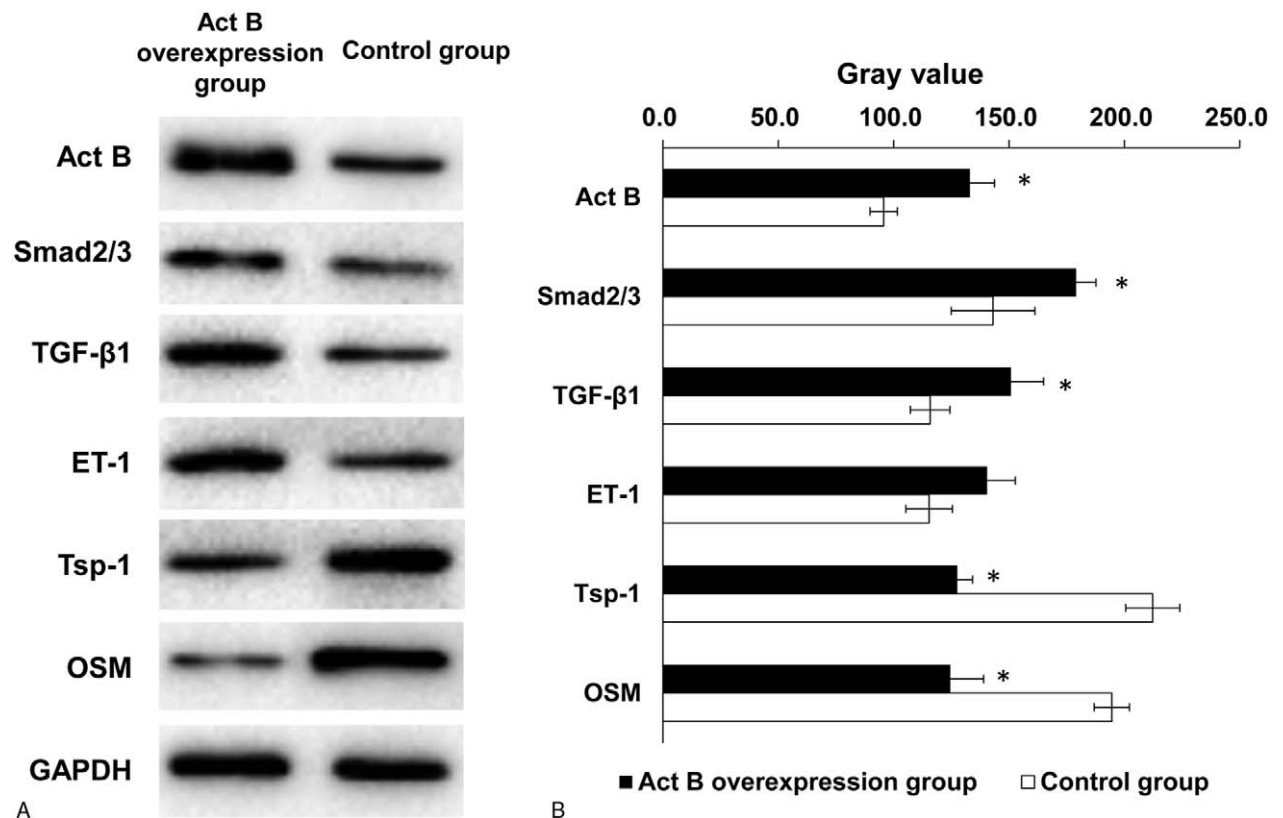

Figure 6. The effect of Act B overexpression on the related protein expressions. (A) Protein bands detected by Western blot after the treatment with rh-Act B. (B) The gray values of the protein bands. $^*P < .05$, compared with the Control group.

also been reported that TGF-β1 plays an important role in the development of benign bile scar.[3,27] In this study, we found that TGF-β1 was differentially expressed in scar fibroblasts. This was further confirmed by ELISA, which found elevated levels of TGF-β1. Our result further verifies that TGF-β1 is an important factor during scar formation.

It is found that fibroblasts can also produce ET-1, which is a potent mitogen for fibroblasts and stimulates the expression of proto-oncogenes such as c-fos and c-myc.[28] ET-1 can act synergistically with a variety of cytokines and play an important role in the development of scars. For example, ET-1 cooperates with TGF-β1 to enhance fibrogenic effects.[29] ET-1 can also cooperate with vascular endothelial growth factor (VEGF) to significantly increase the proliferation, migration, and invasion ability[30] of endothelial cells, and induce neovascularization.[31] In addition, ET-1 can cooperate with basic fibroblast growth factor to promote scar formation.[32] It has also been reported that, the ET level in hypertrophic scar tissue gradually increases, reaches the peak in the proliferative phase, gradually decreases in the remission period, and returned to normal in the mature period, which is consistent with the neovascularization and collagen fiber distribution in the scar tissue at different stages.[33] In this study, the results of the protein chip assay showed that the expression level of ET protein in SCFB cell samples was significantly higher than that of NFB cells, suggesting that the clinical samples obtained in this experiment are in the proliferative phase of bile duct scars.

Tsp-1 is one of the endogenous anti-angiogenic factors, which can inhibit the proliferation and induce the apoptosis of endothelial cells, and inhibit angiogenesis.[34,35] VEGF is the most potent pro-angiogenic factor,[36] while Tsp-1 is a newly discovered factor that strongly inhibits angiogenesis. The expression of VEGF and Tsp-1 is associated with pathological scar formation. VEGF may promote scar hyperplasia by inducing angiogenesis,[37] whereas Tsp-1 inhibits VEGF elevation. The reduction of Tsp-1 will lead to the proliferation of blood vessels in pathological scars, resulting in the formation of pathological scars. It has been reported that[38] the positive rate of Tsp-1 mRNA expression in skin hypertrophic scars and keloids was lower than that in normal skin tissues. Consistently, in the present study, Tsp-1 level was decreased in scar cells by protein chip assay and ELISA validation.

OSM belongs to interleukin-6 (IL-6) family,[39] and can inhibit a variety of tumor cells, such as melanoma cell A375 and lung cancer cell H298.[40] OSM is also involved in the pathophysiological process of liver regeneration.[41] OSM inhibits normal fibroblast apoptosis, promotes normal fibroblast growth, and stimulates collagen secretion.[42] Levy et al[43] reported that OSM level was low in normal liver tissues but increased in liver cirrhosis. In our study, OSM level was also decreased in scar cells than control cells.

Act belongs to TGF-β superfamily,[10] and can promote the differentiation of epithelial cells,[44,45] promote the proliferation of fibroblasts, promote the synthesis of extracellular matrix, and promote the healing of skin wounds. Overexpression of Act causes inflammatory reactions and fibrosis of tissues and organs.[17,46] Some scholars have found that[18,19,47] Act over-expression in transgenic mice can promote skin damage repair, but at the same time it also induces formation of skin scars. Act B stimulates cell proliferation at the site of skin injury and promotes wound healing through the RhoA-Rock-JNK-cJun signaling pathway.[16,48] In this study, protein chip assay showed that Act B

was higher in fibroblasts than in normal fibroblasts. ELISA results also confirmed the results of protein chip assay. By transfecting siRNA-Act B into scar fibroblasts to down-regulate the expression of Act B in SCFBs, the apoptosis of SCFBs increased. The levels of TGF-β1, Smad2/3, and ET-1 decreased, while the levels of Tsp-1 and OSM increased. By contrast, after treatment with rh-Act B, the expression levels of TGF-β1, Smad2/3, and ET-1 were elevated, whereas those of Tsp-1 and OSM decreased. Thus, we suppose that Act B may regulate the expression of the above mentioned proteins, thus playing an important role in the conversion of normal bile duct fibroblasts to scar fibroblasts.

In conclusion, 37 differential proteins were identified from scar fibroblasts. Among them, the proteins associated with scar formation such as Activin B, TGF-β1, ET-1, Tsp-1, and OSM were identified and verified. Activin B signaling plays an important role in the conversion of normal fibroblasts to scar fibroblasts, and TGF-β1, Smad2/3, Tsp-1, and OSM are important participants. This study may provide evidence for the investigating the pathogenesis of benign biliary hypertrophic scar.

Author contributions

Conceived and designed the experiments: Shi-Kang Deng, Jian-Zhong Tang, Yan Jin and Ping-Hai Hu. Performed the experiments: Shi-Kang Deng, Jian-Zhong Tang, Yan Jin, Jun-Feng Wang and Ping-Hai Hu. Analyzed the data: Shi-Kang Deng, Jian-Zhong Tang and Ping-Hai Hu. Contributed reagents/materials/analysis tools: Shi-Kang Deng, Jian-Zhong Tang, Ping-Hai Hu, Jun-Feng Wang and Xiao-Wen Zhang. Wrote the paper: Shi-Kang Deng, Jian-Zhong Tang, Yan Jin, Xiao-Wen Zhang and Ping-Hai Hu. Access to full-text articles: Shi-Kang Deng, Jian-Zhong Tang and Ping-Hai Hu.

References

[1] Costamagna G, Boskoski I. Current treatment of benign biliary strictures. Ann Gastroenterol 2013;26:37–40.

[2] Cote GA, Slivka A, Tarnasky P, et al. Effect of covered metallic stents compared with plastic stents on benign biliary stricture resolution: a randomized clinical trial. JAMA 2016;315:1250–7.

[3] Geng ZM, Zheng JB, Zhang XX, et al. Role of transforming growth factor-beta signaling pathway in pathogenesis of benign biliary stricture. World J Gastroenterol 2008;14:4949–54.

[4] Liu JY, Li SR, Ji SX. [Expression of connective tissue growth factor gene in the hypertrophic scar and keloid tissue]. Zhongguo Xiu Fu Chong Jian Wai Ke Za Zhi 2003;17:436–8.

[5] Siqueira OHK, Oliveira KJ, Carvalho ACG, et al. Effect of tamoxifen on fibrosis, collagen content and transforming growth factor-beta1, -beta2 and -beta3 expression in common bile duct anastomosis of pigs. Int J Exp Pathol 2017;98:269–77.

[6] Li LJ, Wang XY, Zhang P. Expression and significance of TGF-β1 and CTGF in the repairing process of bile duct ischemic injury. J Hepatopancreatobil Surg 2011;23:336–9.

[7] Carlson E, Zukoski CF, Campbell J, et al. Morphologic, biophysical, and biochemical consequences of ligation of the common biliary duct in the dog. Am J Pathol 1977;86:301–20.

[8] Yetti H, Naito H, Yuan Y, et al. Bile acid detoxifying enzymes limit susceptibility to liver fibrosis in female SHRSP5/Dmcr rats fed with a high-fat-cholesterol diet. PLoS One 2018;13:e0192863.

[9] Zhou M, Learned RM, Rossi SJ, et al. Engineered FGF19 eliminates bile acid toxicity and lipotoxicity leading to resolution of steatohepatitis and fibrosis in mice. Hepatol Commun 2017;1:1024–42.

[10] Lin SY, Morrison JR, Phillips DJ, et al. Regulation of ovarian function by the TGF-beta superfamily and follistatin. Reproduction 2003;126:133–48.

[11] Abe Y, Minegishi T, Leung PC. Activin receptor signaling. Growth Factors 2004;22:105–10.

[12] Attisano L, Wrana JL, Montalvo E, et al. Activation of signalling by the activin receptor complex. Mol Cell Biol 1996;16:1066–73.

[13] Ten DP, Hill CS. New insights into TGF-beta-Smad signalling. Trends Biochem Sci 2004;29:265–73.

[14] Munz B, Tretter Y, Hertel M, Engelhardt F. The roles of actinvins in repair processes of the skin and the brain. Mol Cell Endocrinol 2001;180:169–77.

[15] Hubner G, Alzheimer C, Werner S. Activin: a novel player in tissue repair processes. Histol Histopathol 1999;14:295–304.

[16] Zhang M, Liu NY, Wang XE, et al. Activin B promotes epithelial wound healing in vivo through RhoA-JNK signaling pathway. PLoS One 2011;6:e25143.

[17] Werner S, Alzheimer C. Roles of activin in tissue repair, fibrosis, and inflammatory disease. Cytokine Growth Factor Rev 2006;17:157–71.

[18] Munz B, Smola H, Engelhardt F, et al. Overexpression of activin A in the skin of transgenic mice reveals new activities of activin in epidermal morphogenesis, dermal fibrosis and wound repair. EMBO J 1999; 18:5205–15.

[19] Wankell M, Munz B, Hubner G, et al. Impaired wound healing in transgenic mice overexpressing the activin antagonist follistatin in the epidermis. EMBO J 2001;20:5361–72.

[20] Eyden B. Fibroblast phenotype plasticity: relevance for understanding heterogeneity in "fibroblastic" tumors. Ultrastruct Pathol 2004;28:307–19.

[21] Wang XH, Wang Y, Jiang T, et al. Primary culture and biological characteristics of human skin fibroblasts. J China Med Univ 2010; 39:1041–4.

[22] Wu YF, Li TZ, Wu Q, et al. Ultrastructural studies on the fibroblasts of hypertrophic burn scars. J Chin Electron Microsc Soc 2004;23:112–5.

[23] Zhao B, Guan H, Liu JQ, et al. Hypoxia drives the transition of human dermal fibroblasts to a myofibroblast-like phenotype via the TGF-Î²1/ Smad3 pathway. Int J Mol Med 2017;39:153–9.

[24] Jiang H, Zhang L, Yu Y, et al. A pilot study of angiogenin in heart failure with preserved ejection fraction: a novel potential biomarker for diagnosis and prognosis? J Cell Mol Med 2014;18:2189–97.

[25] Wang L, Zhang XX. Expressions and significance of TGF-β_1 and TβR I in benign biliary stricture. J Fourth Mil Med Univ 2007;28:45–7.

[26] Wu Q, He XD, Tao LY, et al. Molecular research progress of mechanism of benign bile duct stenosis. J Hepatopancreatobil Surg 2010;22:80–2.

[27] Li JJ, Li T, Meng YP, et al. Significance of expression of TGF-1 and MMP1 in bile duct injury caused by electrocautery in rabbits. World Chin J Digestol 2013;21:3097–101.

[28] Komuro I, Kurihara H, Sugiyama T, et al. Endothelin stimulates c-fos and c-myc expression and proliferation of vascular smooth muscle cells. FEBS Lett 1988;238:249–52.

[29] Shi-Wen X, Kennedy L, Renzoni EA, et al. Endothelin is a downstream mediator of profibrotic responses to transforming growth factor beta in human lung fibroblasts. Arthritis Rheum 2010;56:4189–94.

[30] Salani D, Taraboletti G, Rosanò L, et al. Endothelin-1 induces an angiogenic phenotype in cultured endothelial cells and stimulates neovascularization in vivo. Am J Pathol 2000;157:1703–11.

[31] DiPietro LA. Angiogenesis and scar formation in healing wounds. Curr Opin Rheumatol 2013;25:87–91.

[32] Yan G, Wei HE. Expression of Endothelin-1 and bFGF mRNA in Keloid Tissues. Chin J Dermatol 2000;33:259–60.

[33] Xiang J, Wang XQ, Liu YK, et al. Expression of ET-1 in fibroblasts, angiogenesis and collagen distributions in scars after burn injury. J Shanghai Jiaotong Univ 2010;30:839–42.

[34] Bornstein P. Thrombospondins as matricellular modulators of cell function. J Clin Invest 2001;107:929–34.

[35] Nesselroth SM, Willis AI, Fuse S. The C terminal domain of thrombospin-1 induces vascular smooth muscle cell chemotaxis. J Vasc Surg 2001;33:595–600.

[36] Johnson KE, Wilgus TA. Vascular endothelial growth factor and angiogenesis in the regulation of cutaneous wound repair. Adv Wound Care (New Rochelle) 2014;3:647–61.

[37] Zhang YM, Fan DL. Advances in research of pathological scar angiogenesis. Chin J Plast Surg 2008;24:246–9.

[38] Qian L, Zhao BC, Li PI, et al. Study of expression of TSP-1 mRNA and MVC in scar tissues. China J Mod Med 2004;14:21–4.

[39] Stobbe-Maicherski N, Wolff S, Wolff C, et al. The interleukin-6-type cytokine oncostatin M induces aryl hydrocarbon receptor expression in a STAT3-dependent manner in human HepG2 hepatoma cells. FEBS J 2013;280:6681–90.

[40] Qin YXZ, Inhibin M. A Novel tumor suppressor. J Int Oncol 1994; 1994:212–6.

[41] Peng JC, Chang XM. Research progress in the relationship between inhibin M and liver regeneration and liver diseases. World Chin J Digestol 2012;20:3725–31.

[42] Scaffidi AK, Mutsaers SE, Moodley YP, et al. Oncostatin M stimulates proliferation, induces collagen production and inhibits apoptosis of human lung fibroblasts. Br J Pharmacol 2002;136:793–801.

[43] Levy MT, Trojanowska M, Reuben A. Oncostatin M: a cytokine upregulated in human cirrhosis, increases collagen production by human hepatic stellate cells. J Hepatol 2000;32:218–26.

[44] Deng M, Chen WL, Takatori A, et al. A role for the mitogen-activated protein kinase kinase kinase 1 in epithelial wound healing. Mol Biol Cell 2006;17:3446–55.

[45] Zhang L, Wang W, Hayashi Y, et al. A role for MEK kinase 1 in TGF-beta/activin-induced epithelium movement and embryonic eyelid closure. EMBO J 2003;22:4443–54.

[46] Jones KL, de Kretser DM, Patella S, et al. Activin A and follistatin in systemic inflammation. Mol Cell Endocrinol 2004;225:119–25.

[47] Sulyok S, Wankell M, Alzheimer C, et al. Activin: an important regulator of wound repair, fibrosis, and neuroprotection. Mol Cell Endocrinol 2004;225:127–32.

[48] Sun L, Wang XE, Zhang M, et al. The treatment of skin wound healing of rats by different transplantation approaches of BMSCs combination with Activin B. Chinese J Clin Anat 2012;30:197–202.